Characteristics of Upstream and Downstream Plasma Parameters from Langmuir Probes and Visible Spectrometers in the D-Module of GAMMA 10/PDX*)

Takaaki IIJIMA, Toshiki HARA, Kunpei NOJIRI, Akihiro TERAKADO, Md. Shahinul ISLAM, Tsubasa YOSHIMOTO, Sotaro YAMASHITA, Naomichi EZUMI, Mizuki SAKAMOTO and Yousuke NAKASHIMA

Plasma Research Center, University of Tsukuba, Tsukuba 305-8577, Japan

(Received 30 September 2018 / Accepted 3 June 2019)

Plasma parameters in the upstream and downstream regions in the divertor simulation experimental module (D-module) of the tandem mirror plasma device GAMMA 10/PDX were conducted using Langmuir probes. The detached plasma was produced using hydrogen puffing. In the upstream region, the electron temperature decreased from 30 to 7 eV, and the electron density increased. On the other hand, rollover of n_e at the V-shaped corner was observed in the downstream region. Increasing H_α/H_β at the corner of the V-shaped target was attributed to the molecular activated recombination processes. H_α/H_β in the downstream region was different from that in the upstream region. Therefore, the ionization front appeared in the upstream region of the D-module.

Keywords: divertor, detached plasma, molecular activated recombination, GAMMA 10/PDX

DOI: 10.1585/pfr.14.2401156

1. Introduction

In a magnetic confinement fusion device, it is important to reduce the particle and heat load on the divertor plate. The production of detached plasma mitigates the particle and heat load [1,2]. Volumetric recombination processes are essential to produce detached plasma. When the electron temperature decreases below a certain value and the electron density is sufficiently high, electron-ion recombination (EIR) occurrs. The EIR is characterized by line emission from high excitation levels and continuum emission [3, 4]. The detached plasmas have been observed in all kinds of devices [4–7]. Molecular activated recombination (MAR) is also an important process for detached plasma production [8–10]. The MAR processes are described as follows [11]:

$$\text{DA-MAR} \quad \text{DA: } H_2(v) + e \rightarrow H^- + H, \tag{1}$$

$$\text{MN: } H^- + H^+ \rightarrow H + H(n = 2, 3), \tag{2}$$

$$\text{IC-MAR} \quad \text{IC: } H_2(v) + H^+ \rightarrow H_2^+ + H, \tag{3}$$

$$\text{DR: } H_2(v)^+ + e \rightarrow H + H(n > 2). \tag{4}$$

The first reaction is the dissociative attachment (DA) of vibrationally excited hydrogen molecules, followed by mutual neutralization. The second reaction is atomic and molecular ion conversion (IC), followed by dissociative recombination.

In GAMMA 10/PDX, the divertor simulation experimental module (D-module) is installed in the west end region, and divertor plasma physics is studied by utilizing end-loss plasma as a divertor simulation plasma [12]. Decrease in the electron temperature and the density rollover with increase in gas pressure is observed in the D-module. It was reported that sources of H_α are both processes of DA-MAR and IC-MAR, and a source of H_β is only IC-MAR from the viewpoint of comparison between H_α and H_β that are caused by the MAR processes [13].

Understanding generating mechanisms of the detached plasma because of the MAR processes and its spatial distribution properties are important to handle heat and particle load in a magnetic confinement fusion reactor. In this study, we perform experiments of hydrogen injection into the divertor simulation plasma in the D-module of GAMMA 10/PDX. The ion saturation current, the electron temperature and density are measured using Langmuir probes that are installed in the upstream and the downstream region of D-module. The atomic emission intensities are observed using spectrometers.

2. Experimental Setup

The experiments were performed in GAMMA 10/PDX [14, 15]. GAMMA 10/PDX is the largest tandem mirror device and consists of four sections, which are central cell, anchor cells, plug/barrier cells and end regions. In GAMMA10/PDX, divertor simulation experiments were

author's e-mail: iijima@prc.tsukuba.ac.jp

*) This article is based on the presentation at the 12th International Conference on Open Magnetic Systems for Plasma Confinement (OS2018).

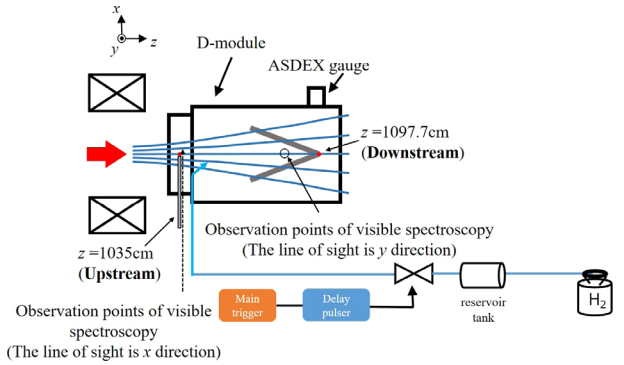

Fig. 1 Schematic of the D-module and its gas line system.

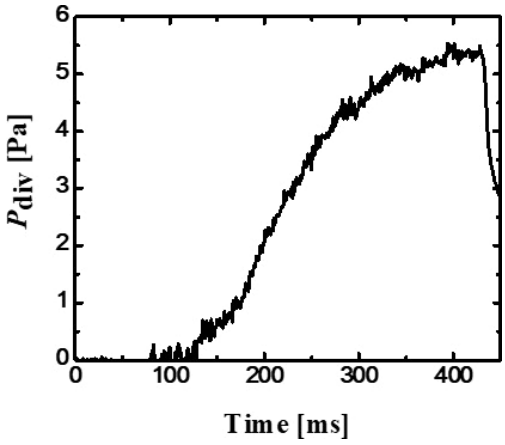

Fig. 2 Time evolution of the neutral gas pressure in the D-module.

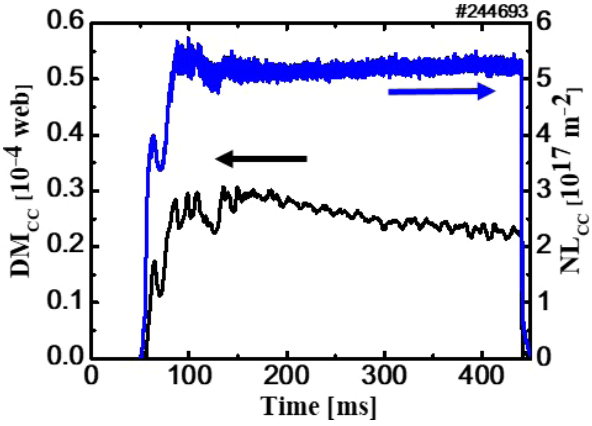

Fig. 3 Time evolution of diamagnetism and electron line density at the central cell.

conducted using the D-module. The D-module can be moved up and down using an elevation system and positioned on axis close to the end-mirror exit in the divertor simulation experiment.

The plasma was generated and heated using ion cyclotron range of frequencies (ICRF) together with gas puffing in the central cell, and the end loss plasma reached the D-module at the west end cell. The D-module comprised a rectangular chamber (cross-section 50×50 cm and length 100 cm) made of stainless steel and V-shaped target equipped with electrostatic probes. Figure 1 shows a schematic of the D-module and its gas line system.

Cold gas (hydrogen) were injected from the gas line, which is located at the inlet of the D-module in order to achieve plasma detachment. The quantity of gas injection was adjusted by changing the plenum pressure of the gas reservoir tank. The visible spectrum, electron density and temperature were measured using spectrometers and Langmuir probes. A single probe was newly installed at z = 1035 cm to measure the plasma parameters of the upstream region of the D-module. To measure the plasma parameters of downstream region, a single probe is installed at the corner of the V-shaped to measure the plasma parameters in the downstream region. target. An optical fiber equipped with lens was installed in the shaft of the probe at z = 1035 cm to measure the visible spectra. The emission intensities were assumed to be from the plasma center even though the plasma has a radial distribution.

3. Results and Discussion

In this study, the plasma parameters in the upstream and downstream regions in the D-module under the detached condition were measured. Hydrogen plasma was generated and heated by ICRF together with gas puffing in the central cell at t = 50 ms. The plasma was maintained for 400 ms.

The gas puffing in the D-module started at 60 ms, and the pulse duration of gas puffing was 0.5 s for 800 mbar of the plenum pressure.

Figure 2 shows a typical characteristic of neutral gas pressure in the D-module by using the ASDEX gauge at a plenum pressure of 750 mbar. Neutral gas was not achieved at the neutral gas at a plenum pressure of 800 mbar. However, no major differences was observed, regardless of 750 and 800 mbar.

The neutral pressure increased with lapse of time due to gas injection. The temporal evolution of (a) diamagnetic signal (DM_{CC}) and (b) electron line density (NL_{CC}) in the central cell is shown in Fig. 3. The plasma increased from 50 ms and reached almost flat at 100 ms. DM_{CC} slightly decreases and NL_{CC} was stable. These parameters were not affected during gas injection. Figure 4 shows the temporal evolution of electron line density (NL_{WP}) at the west plug cell. NL_{WP} is strongly influenced by the gas puffing in the D-module. A part of hydrogen gas that flowed out of the D-module diffused to the west plug cell, and was ionized there.

Figure 5 (a) shows the time evolution of electron temperature in the upstream and downstream regions. The electron temperature in the upstream region T_e^{up} decreased

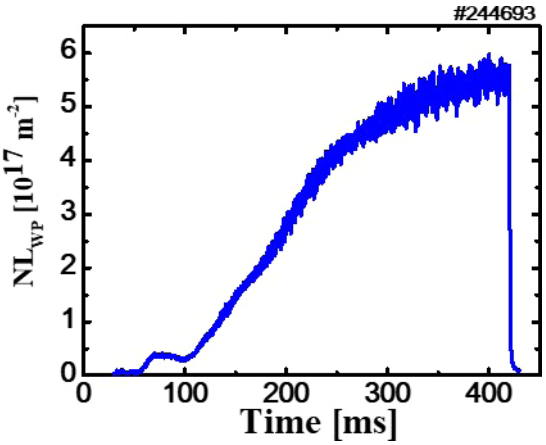

Fig. 4 Time evolution of electron line density at the plug cell.

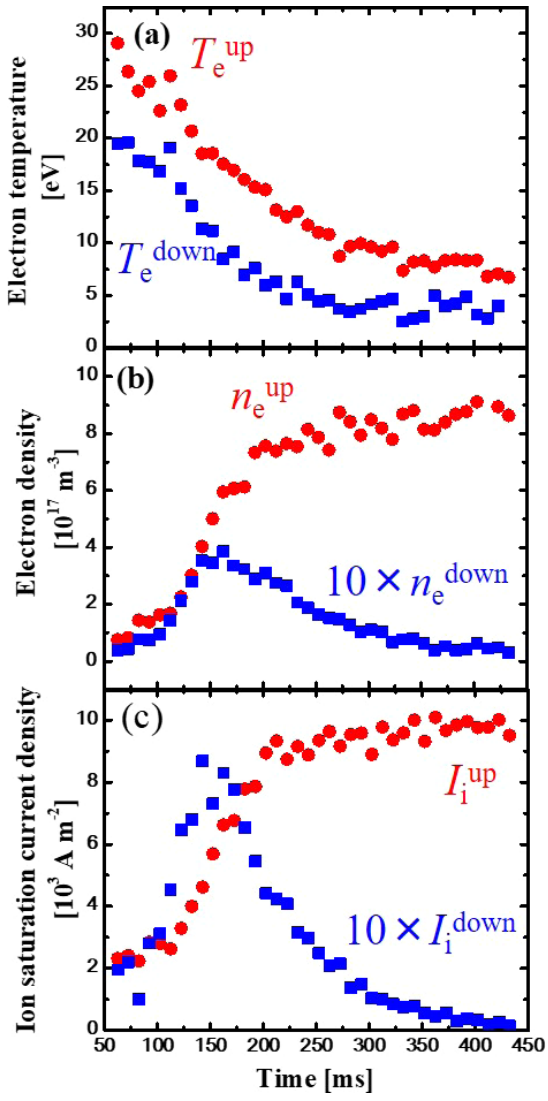

Fig. 5 Time evolution of (a) electron temperature, (b) electron density, and (c) ion saturation current.

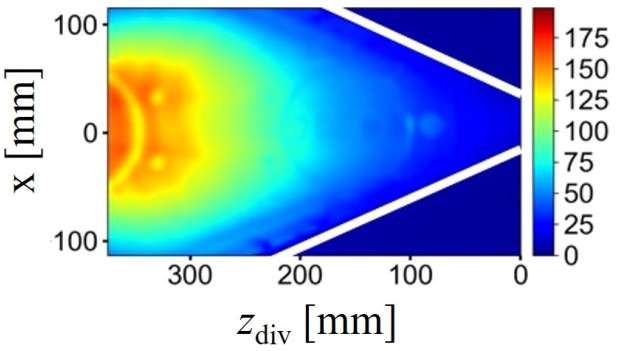

Fig. 6 Two dimensional H_α distribution in the D-module.

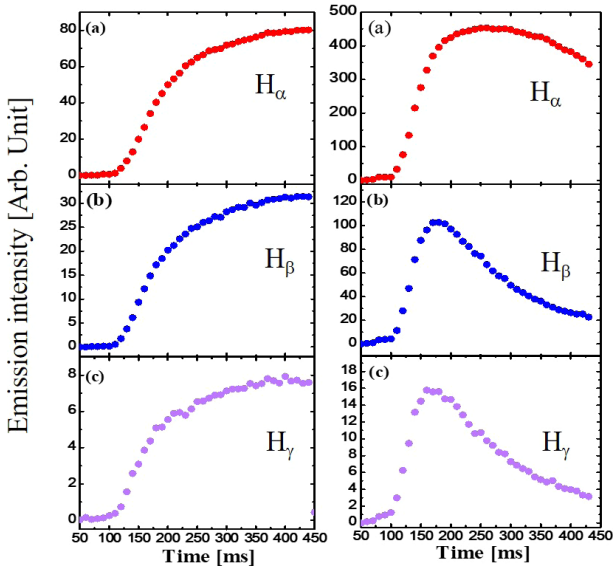

Fig. 7 Time evolution of (a) H_α (b) H_β (c) H_γ in the upstream region and (d) H_α (e) H_β, and (f) H_γ in the downstream region.

from ~30 to ~7 eV as time increased, whereas that in the downstream region T_e^{down} decreased from ~20 to ~2 eV. Here, the cooling rate is defined by $\Delta T/T_{final} = (T_{initial} - T_{final})/T_{final}$, where $T_{initial}$ and T_{final} are the reflect the electron temperature at t = 62.4 ms and t = 432.4 ms, respectively. $\Delta T/T_{final}$ of the upstream region is 3.285, and that of the upstream region is 9. Thus, it is more cooled than upstream T_e^{up}. Figure 5 (b) shows the time evolution of electron density in the upstream and downstream regions. The electron density in the upstream region n_e^{up} increased with lapse of time. It is considered that T_e^{up} depends on the neutral gas pressure in the D-module. On the other hand, the electron density in the downstream region n_e^{down} increased and then decreased. The expansion of flux tube between the upstream and downstream is about 9 times. The electron density reduction was due to gas injection. The density rollover was observed in the downstream region.

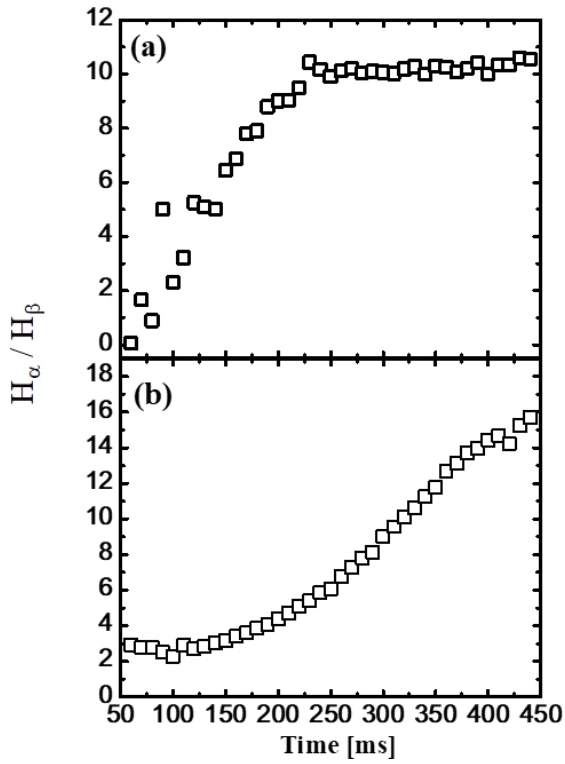

Fig. 8 Time evolution of H_α/H_β in the (a) upstream and (b) downstream regions.

Figure 5 (c) shows the time evolution of the ion current density. The trend of the ion current density was similar to the characteristics of electron density.

Figure 6 shows the two dimensional image of H_α intensity as average of 320 - 330 ms. The dark region appeared at the corner of the V-shaped target. These results indicated that the detached plasma was produced in the downstream region of the D-module.

Balmer line intensities in the upstream and downstream regions are shown in Figs. 7 (a) - (f). In the upstream region, the tendency of Balmer line emission intensities (H_α, H_β, H_γ) was similar to n_e^{up}. Therefore, it is considered that these line emission intensities increased due to the electron density. In the downstream region, the tendency of H_β and H_γ was also similar to n_e^{down}. However, the trend of H_α in the downstream region differed from the tendency of H_α and H_γ.

Figures 8 (a) and (b) show H_α/H_β in the upstream and downstream regions. In 50 - 200 ms, H_α/H_β increased because the plasma parameters changed in this period. Thus ionization and dissociation may proceed. In 200 - 450 ms, the plasma became a steady state. The trend of H_α/H_β in the downstream region differed from that in the upstream region. DA-MAR was assumed dominant compared with IC-MAR [15] for t = 200 - 450 ms, where T_e and n_e decreased considerably. Increasing H_α/H_β indicated that the detached plasma was produced due to MAR processes in the downstream region.

4. Summary

To clarify the characteristics of detached plasma due to the MAR, we investigated plasma parameters in the upstream and downstream regions in the D-module of GAMMA 10/PDX. In the upstream region, T_e decreased from 30 to 7 eV; n_e increased and saturated. Meanwhile, the rollover of n_e at the V-shaped corner was observed, and an ionization front appeared in the upstream region. The trend of H_α/H_β differed from that of the upstream region. In the upstream region, an ionization front formed. In the downstream region, it indicates that H_α increased via excited atoms produced by MAR processes.

In the future, we plan to use the two-point model, which considers the divergent magnetic fields. A probe measurement system will be installed at more upstream region.

Acknowledgments

This work is performed with the support of NIFS Collaborative Research Program (NIFS17KUGM127).

[1] G.F. Matthews, J. Nucl. Mater. **220-222**, 104 (1995).
[2] S. Takamura *et al*., Plasma Sources Sci. Technol. **11**, A42 (2002).
[3] K.J. Gibson *et al*., J. Nucl. Mater. **313**, 1253 (2003).
[4] D. Lumma *et al*., Phys. Plasmas **4**, 2555 (1998).
[5] K. Fujimoto *et al*., Plasma Fusion Res. **4**, 025 (2009).
[6] M.E. Fenstermacher *et al*., Plasma Phys. Control. Fusion **41**, A345 (1999).
[7] G.M. McCracken *et al*., J. Nucl. Mater. **266-269**, 37 (1999).
[8] S.I. Krasheninnikov *et al*., Phys. Plasmas **4**, 1638 (1998).
[9] N. Ohno *et al*., Phys. Rev. Lett. **81**, 818 (1998).
[10] J.L. Terry *et al*., Phys. Plasmas **5**, 1759 (1998).
[11] S.I. Krasheninnikov *et al*., Phys. Lett. **A214**, 285 (1996).
[12] Y. Nakashima *et al*., Fusion Sci. Technol. **63**, 100 (2013).
[13] M. Sakamoto *et al*., Nucl. Mater. Energy **12**, 1004 (2017).
[14] Y. Nakashima *et al*., Nucl. Fusion **57**, 116033 (2017).
[15] M. Sakamoto *et al*., Fusion Sci. Technol. **63**, 188 (2013).